Computers, Materials & Continua CMC, vol.62, no.1, pp.365-383, 2020

Optimization Design of RC Ribbed Floor System Using Eagle Strategy with Particle Swarm Optimization

Jiejiang Zhu[1, *] and Bolun Zhou[1]

Abstract: The eagle strategy algorithm is combined with particle swarm optimization in this paper. The new algorithm, denoted as the ES-PSO, is implemented by interfacing Etabs structural analysis codes. ES-PSO is used to optimize the RC ribbed floor system, including floor and underground garage roof. By considering the effects of reinforcement, the principle of virtual work is applied to calculate the deflections of components. Construction cost is taken as the objective function and the constraint conditions are required to satisfy. Accordingly, the optimal layout, the optimal sections of the beams and slabs and the corresponding reinforcements are obtained for different column grids. In this investigation, the RC ribbed floor system is optimized according to the Chinese standard, whose column grids are 8.4 m and 8.4 m. The performance of the ES-PSO algorithm is good enough, which can be applied to practical engineering. The paper can also provide a basis for subsequent optimization design of monolithic structures.

Keywords: Eagle strategy, discrete variable, floor system, the principle of virtual work, Optimum design, Random walk.

1 Introduction

The Eagle Strategy (ES) algorithm, which is proposed by Yang et al. [Yang and Deb (2010)], is a two-stage hybrid search method for optimization. The algorithm is inspired by the eagle's hunting strategy during the whole pursuing process for prey. It can be applied to settle various kinds of optimization problems, including constrained, unconstrained and multi-objective problems [Derakhshan and Bashiri (2018)]. Compared with other algorithms, the advantage of ES is that any algorithms can be used at different stages of the search process. This advantage enables it easier to utilize the advantages of different algorithms to create better effects. Another advantage of ES is that a balanced tradeoff between global search which is generally slow and fast local search is achieved so as to accelerate the convergence speed and avoid local optimum as far as possible [Gandomi, Yang, Talatahari et al. (2012); Yang, Deb and He (2013); Yang, Karamanoglu, Ting et al. (2014)].

The principle of virtual work is undoubtedly the foundation for all variational principles of mechanics [Benacquista and Romano (2018)]. In fact, it is the basic tool to study equilibrium and deformation of structures [Como (2017)]. Accordingly, the principle can be used in various engineering fields, such as the field of material [Como (2017)],

[1] Department of Civil Engineering, Shanghai University, Shanghai, 200444, China.

[*] Corresponding Author: Jiejiang Zhu. Email: zhujjt@126.com.

continuum physics [Lecoutre, Daher, Devel et al. (2017)], robotic system [Khadiv, Ezati and Moosavian (2017)] and dynamics [Kalani, Rezaei and Akbarzadeh (2016); Pedrammehr, Nahavandi and Abdi (2018); Xin, Deng and Zhong (2016)]. As for civil engineering, the principle of virtual work can be applied as structural optimization method to truss and frame structures to satisfy both stress and displacement constraints [Chan (1992); Makris and Provatidis (2002)]. The principle plays a leading role in the optimization process.

Moreover, the application and research of composite structures are active fields in the study of civil engineering. Different optimization methods play crucial roles in the investigation. With the use of non-uniform rational B-spline (NURBS) functions, the gradient-based optimization has been improved to optimize fiber distribution of fiber-reinforced composite (FRC) materials [Ghasemi, Brighenti, Zhuang et al. (2014)] and sandwich beams with polymeric core [Ghasemi, Kerfriden, Bordas et al. (2015a)]. On the basis of NURBS functions, reliability-based design optimization (RBDO) is presented for cooling channels made of ceramic matrix composite (CMC) [Ghasemi, Kerfriden, Bordas et al. (2015b)]. Topology optimization with combination of isogeometric analysis (IGA), level set method (IS) and pointwise density mapping techniques is presented for design of composite flexoelectric structures [Ghasemi, Park, Alajlan et al. (2018); Ghasemi, Park and Rabczuk (2017); Ghasemi, Park and Rabczuk (2018)].

In traditional design, structural engineers rely on their experience to design a ribbed floor system. Accordingly, it is hard to obtain the optimal design of the ribbed floor system. This paper describes a new hybrid algorithm which combines eagle strategy and particle swarm optimization to address the problem. The algorithm is referred to the ES-PSO algorithm in the rest of the paper and it is implemented by interfacing Etabs structural analysis codes. The principle of virtual work is utilized for the evaluation of the deformation by taking account of the influence of reinforcement. The algorithm is used to optimize the cross sections and the reinforcements of beams and slabs when the construction cost is taken as the objective function. The calculation of construction costs for diverse plane layouts are completed automatically. Consequently, the characteristics of optimization design are automatic iterative computation and short optimization time. It appears that this new algorithm is effective and suitable for structural optimization.

2 Computational theory

2.1 Eagle strategy combined with particle swarm optimization

The ES algorithm uses a combination of crude global search and intensive local search exploiting various algorithms to satisfy different demands. It originates from the eagle's pursuing process for prey in nature and the pursuing process includes the roaming stage and chasing stage. In the roaming stage, the eagle explores a wide range of sparse areas. In the chasing stage, the eagle chases at the top speed once the prey is located. The method seeks the fusion of two entirely distinct algorithms, while the one in the first stage explores large search areas and the one in the second stage adopts highly active search steps.

In the first stage, the Lévy walk is performed as a random search to generate solutions in the search domain. Compared with simple random-walk exploration, Lévy walk is far

more efficient and effective [Yang and Deb (2010)]. The expression is shown by Eq. (1) [Talatahari, Gandomi, Yang et al. (2015)]:

$$X_i^t = X^* + \gamma L(u), L(u) \sim \frac{\beta\Gamma(\beta)\sin(\pi\beta/2)}{\pi}\frac{1}{u^{1+\beta}} \tag{1}$$

where X^* is the current best solution, γ is scaling factor which is taken as 0.01; ~ means that $L(u)$ meets Lévy distribution when step sizes are big enough with the exponent β as 1.2, Γ ( ) is the standard gamma function.

Particle Swarm Optimization (PSO) algorithm is applied as a local search algorithm in the second stage during the optimization process. The PSO algorithm, proposed by Kennedy et al. [Kennedy and Eberhart (1995)], is capable of solving complex optimization problems efficiently. The success of this algorithm depends on the mechanism of information sharing through individuals to reach a common goal collectively [Ray and Liew (2012)]. Compared with other evolutionary algorithms, the advantages of PSO are its faster convergence speed [Si, De and Bhattacharjee (2014)], easier for implementation and a smaller number of parameters to adjust [Fourie and Groenwold (2002); Kalivarapu, Foo and Winer (2009)]. The movement of the particle is characterized by two vectors which represent its present velocity v and position x. A particle relies on itself and other particles in the swarm to update its position [Ibrahim, Ewees, Oliva et al. (2018)]. The algorithm can be represented in the expressions as follows [Clerc and Kennedy (2002)]:

$$\begin{cases} v_{t+1} = \chi\left(\omega v_t + \phi_1 r_{1t}(p_l - x_t) + \phi_2 r_{2t}(p_g - x_t)\right) \\ x_{t+1} = x_t + v_{t+1} \end{cases} \tag{2}$$

where v_t and v_{t+1} are the t-th and (t+1)-th velocities, x_t and x_{t+1} are the t-th and (t+1)-th particle positions, χ is constriction coefficient, ω is the inertia weight which is taken as 0.9 initially to improve the speed of convergence [Eberhart and Shi (2000)], ϕ_1 and ϕ_2 are acceleration coefficients, r_{1t} and r_{2t} are random parameters $\in [0,1]$, p_l is the previous best position of particle, p_g is the best position of all swarm,

$$\chi = \frac{2}{\left|2 - \phi - \sqrt{\phi^2 - 4\phi}\right|} \tag{3}$$

where $\phi = \phi_1 + \phi_2$ and $\phi > 4$.

Fig. 1 presents the flow chart of ES-PSO algorithm.

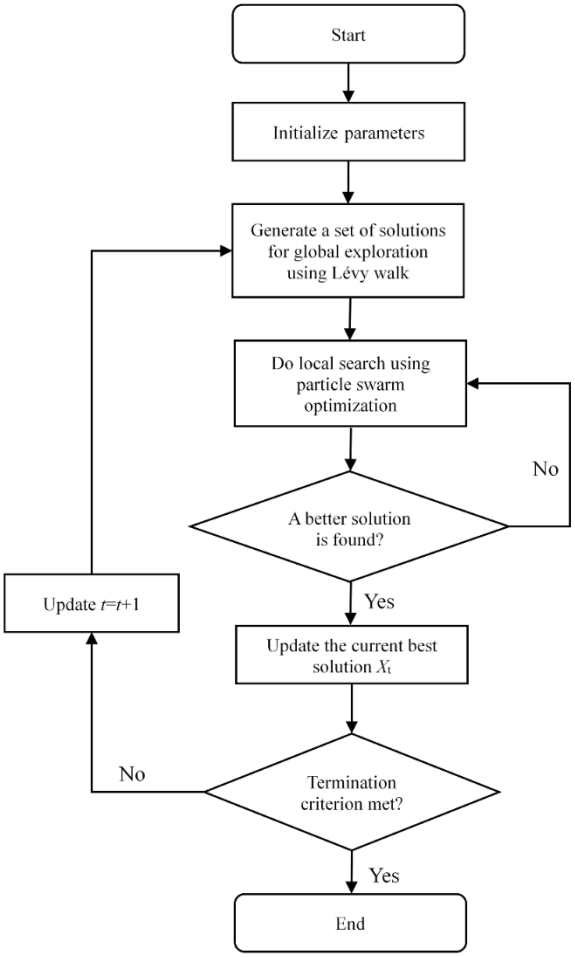

Figure 1: Flow diagram of ES-PSO algorithm

2.2 The principle of virtual work

The deformation of deformable structures occurs as structural members are subjected to different actions, such as various external loads, settlements of supports, change of temperature, and fabrication errors [Karnovsky and Lebed (2010)]. External loads act on the deformable structures, which cause internal forces and deflection. The member *i* causes the deflection at a point is defined as that member's deflection contribution δ_i. The degree of contribution is dominated by the member's internal forces and stiffness [Elvin and Strydom (2018); Walls and Elvin (2010)]. A unit load is applied to the structure at the critical point where the deflection has to be restricted. The unit load creates the unit state and the real load creates the actual state. The total deflection is calculated at the critical point by the summation of all members' deflection contribution $\sum \delta_i$.

With the use of the principle of work, the deflection contribution of each of the member *i*

is calculated.

$$\delta_i = \int_0^L \frac{M\overline{m}}{B}dx + \int_0^L \frac{T\overline{t}}{GJ}dx + \int_0^L \frac{Q\overline{q}}{GA}dx + \frac{F\overline{f}}{EA}L \tag{4}$$

where B is the flexural rigidity, GJ is the torsional rigidity, GA is the transversal rigidity, EA is the axial rigidity, M are bending moments in actual state; T are torsional moments in actual state; Q are shear forces in actual state; F are axial forces in actual state. $\overline{m}$, $\overline{t}$, $\overline{q}$ and $\overline{f}$ are internal forces (bending, torsional moments, shear and axial forces) in unit state, L is the length of each member.

For 2D structures like beams, Eq. (4) is simplified into Eq. (5). Shear force is neglected because it has little effect on a deflection of beams [Makris, Provatidis and Rellakis (2006)]. Similarly, Axial force is omitted because the lateral load is without consideration.

$$\delta_i = \int_0^L \frac{M\overline{m}}{B}dx \tag{5}$$

Fig. 2 are the bending moment diagrams in actual state and unit state. We assume that $M(x)$ varies linearly with the length of the beam [Makris, Provatidis and Rellakis (2006)]. After the bending moment diagrams are simultaneously segmented into n elements，the calculation of deflection can be converted into:

$$\delta_i = \int_0^L \frac{M\overline{m}}{B}dx = \frac{1}{B}\int_0^L M\overline{m}dx = \sum_{j=0}^{n-1} \frac{L}{6Bn}\left(2m_j \times \overline{m}_j + 2m_{j+1} \times \overline{m}_{j+1} + m_j \times \overline{m}_{j+1} + m_{j+1} \times \overline{m}_j\right) \tag{6}$$

where m_j and m_{j+1} are j-th and (j+1)-th elements of bending moment diagram in an actual state, $\overline{m}_j$ and $\overline{m}_{j+1}$ are j-th and (j+1)-th elements of bending moment diagram in the unit state, n is the number of total elements.

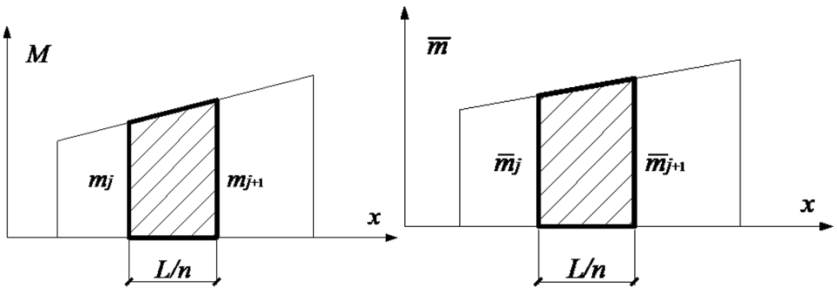

(a) In actual state (b) In unit state

Figure 2: Bending moment diagrams

3 The concept of optimization

3.1 Analysis of the whole schemes

The optimization of the whole schemes is to search for the optimal layout by means of changing the layout of secondary beams. The number of secondary beams in X direction is 0~j and the number of secondary beams in Y direction is 0~k. Accordingly, the

number of all schemes is $(j+k+j\times k+1)$. Fig. 3 presents the plane layout of secondary beams where l_x and l_y are spans in X and Y directions. Based on the principle of the minimum cost, the optimal conditions of each scheme are obtained. At length, the optimal layout is obtained by comparing each scheme separately.

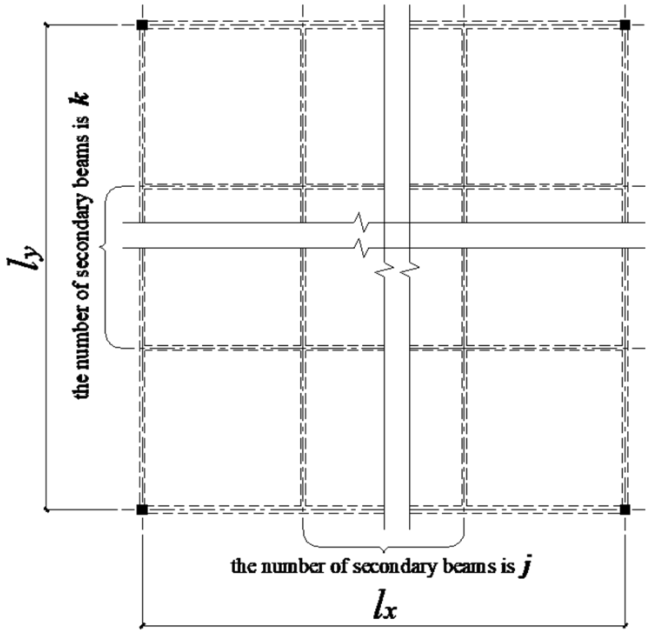

Figure 3: Plane layout of secondary beams

3.2 Optimization design of components

Each component is optimized after integral structural analysis of the floor system is completed. The section of each component is optimized according to the fixed internal forces. The structural analysis is in progress using the updated sections of components so as to obtain new results of internal forces. This process is repeated until the cost difference within two iterations is in convergence. Subsequently, the optimization process is aborted and the optimum result is acquired. Fig. 4 presents the optimization process.

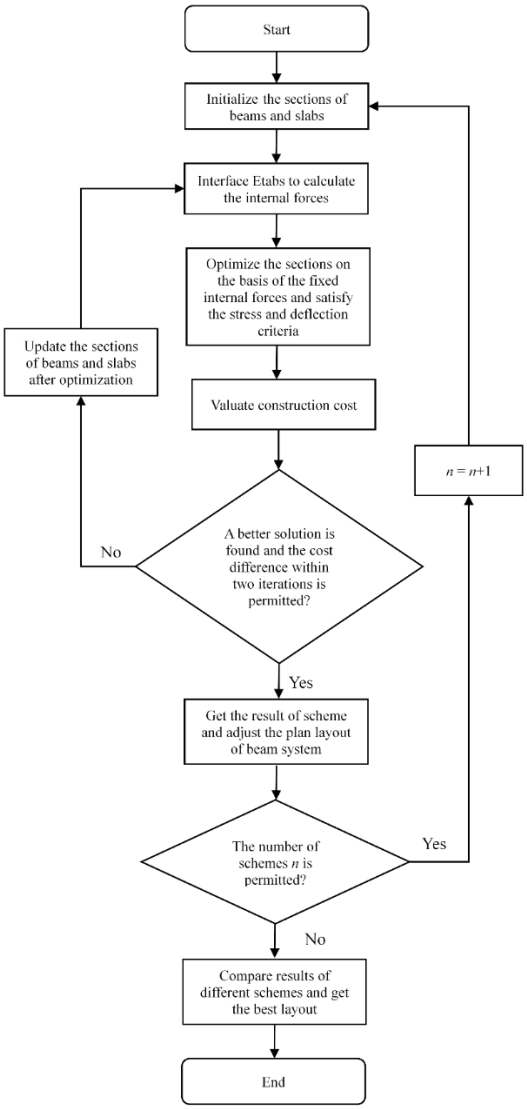

Figure 4: Flow diagram of the optimization process

4 Optimization model

4.1 Objective function and optimum variables

The total cost of the floor system is set as the objective function which includes the cost of beams and slabs. The costs of concrete, formwork and reinforcements are considered and the integrated unit prices of them are calculated on the basis of budget quota.

4.1.1 Objective function of slab

$$C_s = \left(A_{sbx} l_{sy} + A_{sby} l_{sx} + (A_{stx} l_{sy} + A_{sty} l_{sx}) / 2 \right) \cdot \rho_r C_r + h_s l_{sx} l_{sy} C_c + l_{sx} l_{sy} C_f \quad (7)$$

where C_s is the total cost of slab, C_r , C_c and C_f are integrated unit prices of reinforcements, concrete and formwork, h_s is the thickness of slab, ρ_r is density of reinforcements, l_{sx} and l_{sy} are spans of slabs in X and Y directions, A_{stx} , A_{sty} , A_{sbx} and A_{sby} are reinforcement areas per unit length for the top and bottom of slab in X and Y directions, which is shown in Fig. 5.

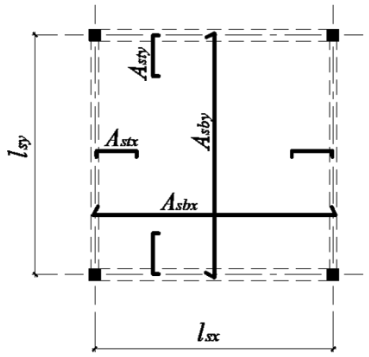

Figure 5: Parametric diagram of reinforcement in slab

4.1.2 Objective function of beam

$$C_b = \sum \left\{ \begin{array}{l} \left[A_{sti} l_{bi} + A_{sc1i} l_{bi} + \frac{2}{3} A_{sc2i} l_{bi} + 2 A_{ssi} \cdot \left(b_{bi} + h_{bi} - 4c \right) \cdot \left(\frac{2 l_{bi}}{3 s_{i1}} + \frac{l_{bi}}{3 s_{i2}} \right) \right] \rho_r C_r \\ + b_{bi} (h_{bi} - h_s) l_{bi} C_c + \left[b_{bi} + 2 (h_{bi} - h_s) \right] l_{bi} C_f \end{array} \right\} \tag{8}$$

where C_b is the total cost of beam, b_{bi} , h_{bi} and l_{bi} is the width, height and the length of beam in *i*-th member, A_{ssi} , A_{sti} , A_{sc1i} and A_{sc2i} are total areas of stirrups, tension reinforcements, compression reinforcements set for the whole beams and the support in *i*-th member, c is the thickness of concrete cover, s_{i1} and s_{i2} are stirrup spacing at the critical section and the other section in *i*-th member.

4.2 Constraint conditions

The structure is required to meet the strength, deflection, crack criteria and the corresponding detailing requirements according to the design code [Ministry of Housing and Urban-Rural Department of the People's Republic of China (2011)]. Thereinto, the deflection of beams is considered to be the primary deflection requirement to be satisfied.

4.2.1 Strength requirements

$$f_c \cdot x = f_y \cdot A_s \tag{9}$$

$$M \le f_y \cdot A_s \cdot (h_0 - \frac{x}{2}) \tag{10}$$

$$x \le \xi_b \cdot h_0 \tag{11}$$

$$\frac{A_s}{h_0} \ge \rho_{\min} \tag{12}$$

where f_c, f_y are concrete cylinder compressive strength and steel yield strength, A_s is the area of longitudinal tension reinforcement, M is the design value of the bending moment, h_0 is the effective depth of the section, x, ξ_b are relative height and bounding relative height of the compression zone, $\rho_{\min}$ is minimum steel ratio.

4.2.2 Deflection requirements

Eq. (6) is applied to calculate the deflection of beams by the use of the principle of virtual work. The flexural rigidity of beam B considers the effect of reinforcement rather than simply the elastic stiffness.

$$B = \frac{E_s A_s h_0^2}{1.15\varphi + 0.2 + \frac{6\alpha_E \rho}{1 + 3.5\gamma_f}} \tag{13}$$

where E_s is the elastic modulus of reinforcement, φ is the nonuniformity coefficient of tension reinforcement strain between cracks which is set as 0.7 for simplicity, α_E is modular ratio, which is the ratio of the reinforcement's and the concrete's modulus of elasticity, ρ is the reinforcement ratio which is set as 0.01 for simplicity, γ_f is the ratio of tensile flange area and web area, which is set as 0 for the rectangle section.

4.2.3 Crack requirements

$$\omega \le \omega_{\max} \tag{14}$$

$$\omega = \alpha_{cr} \cdot \varphi \cdot \frac{\sigma_s}{E_s}(1.9c_s + 0.08\frac{d_{eq}}{\rho_{te}}) \tag{15}$$

$$\rho_{te} = \frac{A_s}{A_{te}} \tag{16}$$

where ω, $\omega_{\max}$ are the crack width and the admissible limit of the width [Ministry of Housing and Urban-Rural Department of the People's Republic of China (2011)], α_{cr} is the characteristic coefficient which is set as 1.9 for bending components, σ_s is the stress in steel under characteristic load combination, c_s is the edge distance measured to the outside edge of tension reinforcement, d_{eq} is the bars diameter of longitudinal tension

reinforcement, ρ_{te} is the reinforcement ratio of effective area, A_{te} is the effective area consisting of $0.5A_c$ and A_c is denoted as the section area of concrete.

4.2.4 Detailing requirements

The sections of beams and slabs are supposed to satisfy detailing requirements. For the case of the underground garage roof and the floor slab, the limits for the sections of beams and slabs are quite different, which is presented in Tab. 1.

Table 1: Section limits for beam and slab (unit: mm)

Case	Slab	Beam		Secondary beam	
	Thickness	Width	Height	Width	Height
Garage roof	250~500	250~500	400~900	200~500	400~800
Floor slab	100~200	250~500	300~700	200~500	300~600

5 Optimization program and results

On account of the ES-PSO algorithm, the optimization program of the ribbed floor system is coded with VB programming language. Etabs structural analysis codes are interfaced repetitively in the optimization process. The process involves automatic modeling, acquisition of the results of internal forces, optimization of the sections, repeated performance of structural analysis with the updated sections, evaluation of the cost and adjustment of the plane layout of beam system. The optimization is operated automatically when some specific parameters are given which includes column grids, loads, the storey height and the maximum number of secondary beams. Fig. 6 presents the optimization program interface. The layout of secondary beams is adjusted automatically and the sections and reinforcements of beams and slabs are optimized in the program. Therefore, the optimal layout of the floor system is obtained. After the optimization, some relevant information can be checked via text files including the internal forces, deflections, the optimal sections and the corresponding reinforcements and the cost of each scheme.

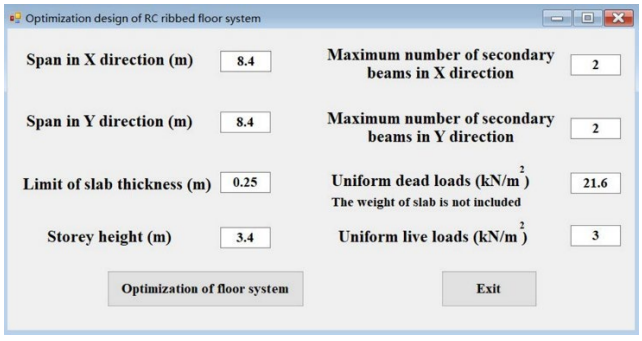

Figure 6: The program interface

5.1 Model simplification

Fig. 7 presents the plane layout of the RC ribbed floor system in practical engineering for general cases. For the convenience of the research, one grid is taken to analyze which is represented as the filled area in Fig. 7. Fig. 8 shows a 3-dimensional model built in Etabs. Two adjustments have been made so that the model in Fig. 8 matches the practical case in Fig. 7. Firstly, the constraints have been set in the supporting positions on both ends of the beam. Hence, the simply-supported beam has turned to both ends continuous beam to meet the actual situation. Secondly, the internal forces of beams are doubled after the internal forces are obtained when calling program. The purpose is to consider the load transmission from the adjacent grids to the beam. Based on these adjustments, the actual situation in Fig. 7 is simplified to the model in Fig. 8.

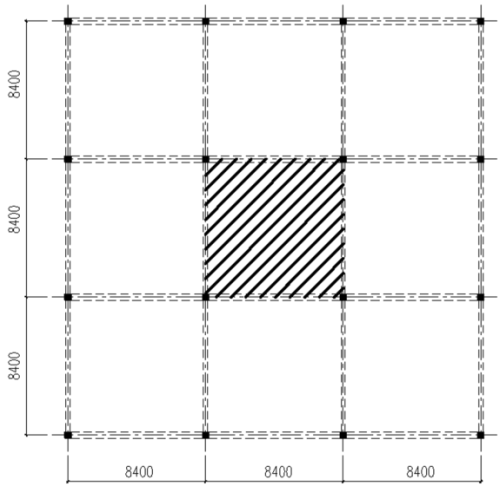

Figure 7: Plane layout of the ribbed floor (unit: mm)

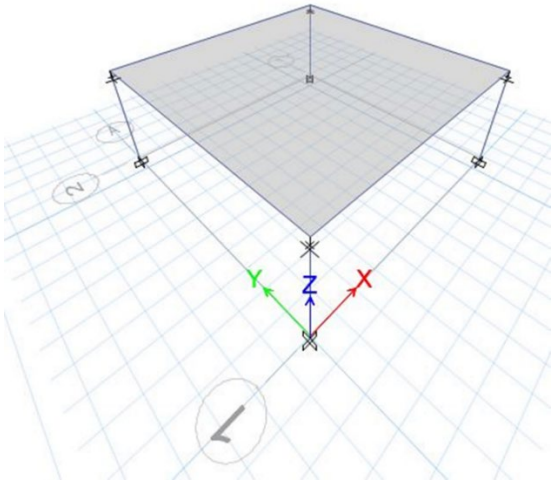

Figure 8: 3D view of Etabs model

5.2 Underground garage roof

5.2.1 Project profile

The column grids of the floor system are 8.4 m and 8.4 m, and 3-dimensional view of Etabs model is shown in Fig. 8. The maximum number of secondary beams in both directions is two. Thus, Fig. 9 presents the plane layouts of beam system in all cases and Fig. 9(a) presents the sections of beams and slabs before optimization. The storey height of the garage roof is 3.4 m. The uniform dead load is 21.6 kN/m^2 which is equivalent to 1.2 m covering soils and the live load is 3 kN/m^2. The minimum limit of slab thickness is 250 mm. As the slab is thick enough, the influence of the slab stiffness out of plane is considered when the internal forces of floor system are calculated.

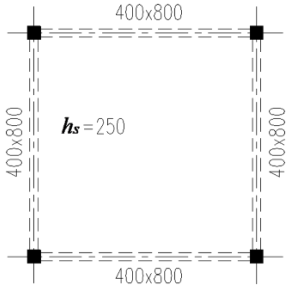

(a) Scheme 1 (no secondary beam in two directions, '0-0' for short)

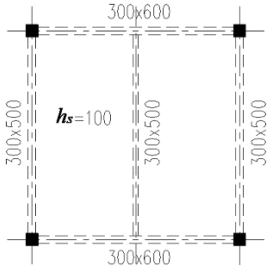

(b) Scheme 2 (one secondary beam in one direction, '0-1' for short)

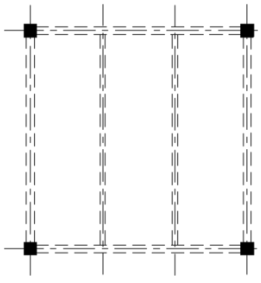

(c) Scheme 3 (two secondary beams in one direction, '0-2' for short)

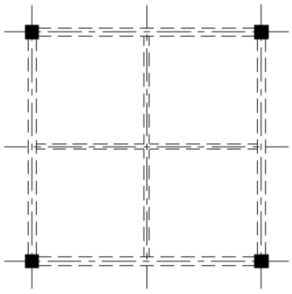

(d) Scheme 4 (one secondary beam in two directions, '1-1' for short)

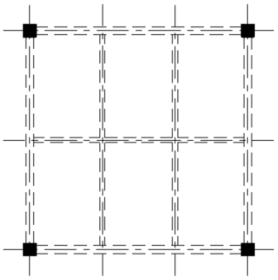

(e) Scheme 5 (one secondary beam in one direction and two secondary beams in the other direction, '1-2' for short)

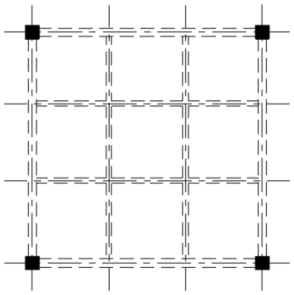

(f) Scheme 6 (two secondary beams in two directions, '2-2' for short)

Figure 9: Plane layout of beam system

Based on the budget quota for Shanghai [Quota management station of Shanghai construction engineering (2001)], Tab. 2 presents the integrated unit price of beam and slab which is used for optimization of the cases below.

Table 2: Integrated unit price of beam and slab

Type of elements	Integrated unit price		
	Concrete ($yuan/m^3$)	Reinforcement (yuan/t)	Formwork ($yuan/m^2$)
Slab	709	5695	84
Beam	708	5710	89

5.2.2 Optimization results of the underground garage roof

Fig. 10 presents the cost of each scheme. Based on these data, we concluded that the optimal layout is the scheme with no secondary beams. Fig. 11 presents the optimal sections of beams and slab.

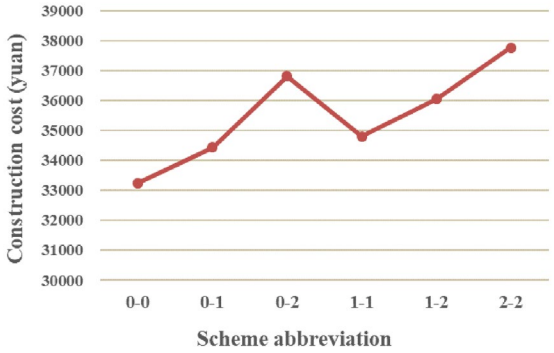

Figure 10: Costs of layout scheme

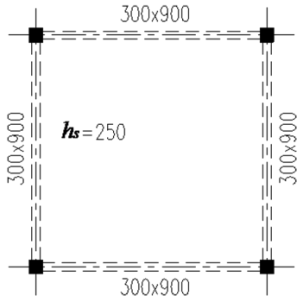

Figure 11: Optimal sections of beam and slab

The results of internal forces and the deflection are compared before optimization and after optimization, which is shown in Tab. 3. According to Tab. 3, a certain increase of internal forces by 1.5%~2.1% acts on beams after optimization. Because beams and slab act on each other in this case, the internal forces of beams augment with the adjustment of sections. However, there is a certain decrease of deflection about 5.94% after optimization.

Table 3: Comparison of internal forces and deflection (bending moment, kNm; shear force, kN; deflection, mm)

The scheme	Beams in X and Y directions			
	Support moment	Midspan moment	Shear force	Deflection
Before optimization	1137.3	739.8	802.3	7.74
After optimization	1160.8	751.4	819.2	7.28

5.3 Floor slab

5.3.1 Project profile

The column grids of the floor system are 8.4 m and 8.4 m. The maximum number of secondary beams in both directions is two. Thus, Fig. 9 presents the plane layouts of beam system in all cases and Fig. 9(b) presents the sections of beams and slabs before optimization. The storey height of the floor is 3 m. The uniform dead load is 2.5 kN/m^2 and the live load is 3 kN/m^2. The minimum limit of slab thickness is 100 mm. As the slab is thin, the influence of the slab stiffness out of plane is out of consideration when the internal forces of floor system are calculated.

5.3.2 Optimization results of floor slab

Fig. 12 presents the cost of each scheme. Based on these data, we concluded that the optimal layout is the scheme with one secondary beam in one direction. Fig. 13 presents the optimal sections of beams and slab.

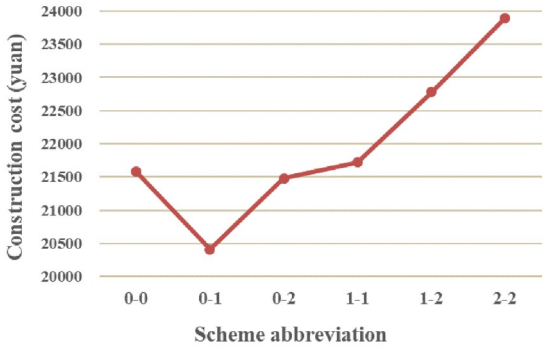

Figure 12: Costs of layout scheme

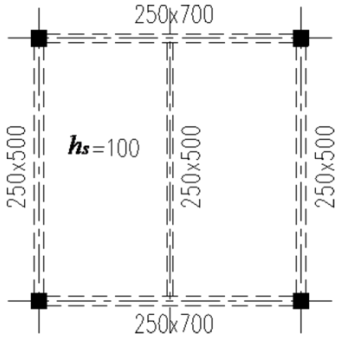

Figure 13: Optimal sections of beam and slab

Tab. 4 and Tab. 5 present the results of internal forces and the deflection before optimization and after optimization. According to Tab. 4, a certain decrease of internal forces by 1.5%~3.5% acts on beams after optimization without regard for slab stiffness

out of a plane in this case.

According to Tab. 5, there is a certain decrease of deflection in beams about 4.87% and 8.56% after optimization with the same circumstance. The reductions of internal forces and deflections embody the role of the optimization.

Table 4: Comparison of internal forces (bending moment, kNm; shear force, kN)

Scheme	Beams in X direction			Beams in Y direction			Secondary beam		
	Support moment	Midspan moment	Shear force	Support moment	Midspan moment	Shear force	Support moment	Midspan moment	Shear force
Before optimization	448.5	409.9	285.8	234.4	148.5	169.9	250.8	133.8	153.8
After optimization	441.2	402.4	281.5	227.1	144.1	163.9	246.4	131.6	150.7

Table 5: Comparison of structure deflection (unit: mm)

The scheme	Beams in X direction	Beams in Y direction	Secondary beam
Before optimization	7.01	11.49	9.9
After optimization	6.41	10.93	10.21

6 Conclusions

The paper presents a two-stage hybrid search method which combines the Eagle Strategy with Particle Swarm Optimization (ES-PSO) for structural optimization. A good balance between crude global search and intensive local search is achieved. Lévy walk is utilized for global search which has been proved highly efficient. Based on the unique mechanism of information sharing, particle swarm optimization is applied to speed up the convergence for local search. Therefore, the excellent performance of ES-PSO is guaranteed by the characteristics mentioned above.

ES-PSO is applied to optimize the RC ribbed floor system including floor and underground garage roof and Etabs analysis codes are interfaced for structural analysis. The information containing the optimal layout and sections, internal forces, the reinforcement and the cost is obtained when construction cost is set as the objective function. In addition, the principle of virtual work is used to check the deflection by considering the factor of reinforcement. The optimization results illustrate the accuracy and efficiency of the algorithm and it can also reduce time consumption in the period of optimization. Accordingly, ES-PSO is an effective way for structural optimization problems.

Further study should analyze other applications of the algorithm. ES-PSO may be utilized to optimize the monolithic structures rather than simply the part of the floor system. The optimization of monolithic structures may reveal the efficiency and the multipurpose of the algorithm. This paper can be regarded as the basis for subsequent monolithic optimization. Another improvement may focus on the sensitivity of ES-PSO by means of related parameters to obtain a better combination of the algorithm. Furthermore, other algorithms for local search may be reliable.

References

Benacquista, M. J.; Romano, J. D. (2018): *Classical Mechanics*. Undergraduate Lecture Notes in Physics, Springer, Cham.

Chan, C. M. (1992): An optimality criteria algorithm for tall steel building design using commercial standard sections. *Structural and Multidisciplinary Optimization*, vol. 5, no. 1, pp. 26-29.

Clerc, M.; Kennedy, J. (2002): The particle swarm-explosion, stability, and convergence in a multidimensional complex space. *IEEE Transactions on Evolutionary Computation*, vol. 6, no. 1, pp. 58-73.

Como, M. (2017): Virtual displacements principle, existence and uniqueness for elastic no tension bodies. *Meccanica*, vol. 52, no. 6, pp. 1397-1405.

Derakhshan, S.; Bashiri, M. (2018): Investigation of an efficient shape optimization procedure for centrifugal pump impeller using eagle strategy algorithm and ANN (case study: slurry flow). *Structural and Multidisciplinary Optimization*, vol. 58, pp. 459-473.

Eberhart, R.; Shi, Y. (2000): Comparing inertia weights and constriction factors in particle swarm optimization. *Proceedings of the 2000 Congress on Evolutionary Computation*, vol. 1, pp. 84-88.

Elvin, A.; Strydom, J. (2018): Optimizing structures with semi‐rigid connections using the principle of virtual work. *International Journal of Steel Structures*, vol. 18, no. 3, pp. 1006-1017.

Fourie, P. C.; Groenwold, A. A. (2002): The particle swarm optimization algorithm in size and shape optimization. *Structural and Multidisciplinary Optimization*, vol. 23, no. 4, pp. 259-267.

Gandomi, A. H.; Yang, X. S.; Talatahari, S.; Deb, S. (2012): Coupled eagle strategy and differential evolution for unconstrained and constrained global optimization. *Computers and Mathematics with Applications*, vol. 63, no. 1, pp. 191-200.

Ghasemi, H.; Brighenti, R.; Zhuang, X.; Muthu, J.; Rabczuk, **T.** (2014): Optimization of fiber distribution in fiber reinforced composite by using NURBS functions. *Computational Materials Science*, vol. 83, pp. 463-473.

Ghasemi, H.; Kerfriden, P.; Bordas, S. P. A. et al. (2015a): Interfacial shear stress optimization in sandwich beams with polymeric core using non-uniform distribution of reinforcing ingredients. *Composite Structures*, vol. 120, pp. 221-230.

Ghasemi, H.; Kerfriden, P.; Bordas, S. P. A.; Jacob Muthu, **S. D.** (2015b): Probabilistic multiconstraints optimization of cooling channels in ceramic matrix composites. *Composites Part B*, vol. 81, pp. 107-119.

Ghasemi, H.; Park, H. S.; Alajlan, N.; Rabczuk, T. (2018): A computational framework for design and optimization of flexoelectric materials. *International Journal of Computational Methods*, vol. 15, no. 3, 1850097.

Ghasemi, H.; Park, H. S.; Rabczuk, T. (2017): A level-set based IGA formulation for topology optimization of flexoelectric materials. *Computer Methods in Applied Mechanics and Engineering*, vol. 313, pp. 239-258.

Ghasemi, H.; Park, H. S.; Rabczuk, T. (2018): A multi-material level set-based topology optimization of flexoelectric composites. *Computer Methods in Applied Mechanics and Engineering*, vol. 332, pp. 47-62.

Ibrahim, R. A.; Ewees, A. A.; Oliva, D.; Abd Elaziz, M.; Lu, S. F. (2018): Improved SALP swarm algorithm based on particle swarm optimization for feature selection. *Journal of Ambient Intelligence and Humanized Computing*, pp. 1-15.

Kalani, H.; Rezaei, A.; Akbarzadeh, A. (2016): Improved general solution for the dynamic modeling of Gough-Stewart platform based on principle of virtual work. *Nonlinear Dynamics*, vol. 83, no. 4, pp. 2393-2418.

Kalivarapu, V.; Foo, J. L.; Winer, E. (2009): Improving solution characteristics of particle swarm optimization using digital pheromones. *Structural and Multidisciplinary Optimization*, vol. 37, no. 4, pp. 415-427.

Karnovsky, I. A.; Lebed, O. (2010): *Advanced Methods of Structural Analysis*. Springer, Boston, MA.

Kennedy, J.; Eberhart, R. (1995): Particle swarm optimization. *Proceedings of IEEE International Conference on Neural Networks*, vol. 4, pp. 1942-1948.

Khadiv, M.; Ezati, M.; Moosavian, S. A. A. (2017): A Computationally efficient inverse dynamics solution based on virtual work principle for biped robots. *Iranian Journal of Science and Technology, Transactions of Mechanical Engineering*, pp. 1-16.

Lecoutre, G.; Daher, N.; Devel, M.; Hirsinger, L. (2017): Principle of virtual power applied to deformable semiconductors with strain, polarization, and magnetization gradients. *Acta Mechanica*, vol. 228, no. 5, pp. 1681-1710.

Makris, P. A.; Provatidis, C. G. (2002): Weight minimisation of displacement-constrained truss structures using a strain energy criterion. *Computer Methods in Applied Mechanics and Engineering*, vol. 191, no. 19, pp. 2187-2205.

Makris, P. A.; Provatidis, C. G.; Rellakis, D. A. (2006): Discrete variable optimization of frames using a strain energy criterion. *Structural and Multidisciplinary Optimization*, vol. 31, no. 5, pp. 410-417.

Ministry of Housing and Urban-Rural Department of the People's Republic of China (2011): *Code for Design of Concrete Structures (GB 50010-2010)*. China Architecture & Building Press, Beijing.

Pedrammehr, S.; Nahavandi, S.; Abdi, H. (2018): Closed-form dynamics of a hexarot parallel manipulator by means of the principle of virtual work. *Acta Mechanica Sinica*, vol. 34, no. 5, pp. 883-895.

Quota Management Station of Shanghai Construction Engineering (2001): *Budget Quota of Construction Engineering and Decoration Engineering (2000)*. Shanghai Popular Science Press, Shanghai.

Ray, T.; Liew, K. M. (2012): A swarm metaphor for multiobjective design optimization. *Engineering Optimization*, vol. 34, no. 2, pp. 141-153.

Si, T.; De, A.; Bhattacharjee, A. K. (2014): Grammatical swarm based-adaptable velocity update equations in particle swarm optimizer. *Advances in Intelligent Systems and Computing*, vol. 247.

Talatahari, S.; Gandomi, A. H.; Yang, X. S.; Deb, S. (2015): Optimum design of frame structures using the eagle strategy with differential evolution. *Engineering Structures*, vol. 91, pp. 16-25.

Walls, R.; Elvin, A. (2010): Optimizing structures subjected to multiple deflection constraints and load cases using the principle of virtual work. *Journal of Structural Engineering*, vol. 136, no. 11, pp. 1444-1452.

Xin, G.; Deng, H.; Zhong, G. (2016): Closed-form dynamics of a 3-DOF spatial parallel manipulator by combining the Lagrangian formulation with the virtual work principle. *Nonlinear Dynamics*, vol. 86, no. 2, pp. 1329-1347.

Yang, X. S.; Deb, S. (2010): Eagle strategy using Lévy walk and firefly algorithms for stochastic optimization. *Studies in Computational Intelligence*, vol. 284, pp. 101-111.

Yang, X. S.; Deb, S.; He. X. (2013): Eagle strategy with flower algorithm. *Proceedings of the 2013 International Conference on Advances in Computing, Communications and Informatics*, pp. 1213-1217.

Yang, X. S.; Karamanoglu, M.; Ting, T.; Zhao, Y. (2014): Applications and analysis of bio-inspired eagle strategy for engineering optimization. *Neural Computing and Applications*, vol. 25, pp. 411-420.